



Hidden but not lost: the larval cranial anatomy of the Majorcan midwife toad (*Alytes muletensis*)

PAUL LUKAS

Institut für Zoologie und Evolutionsforschung mit Phyletischem Museum, Ernst-Haeckel-Haus und Biologiedidaktik,
Friedrich-Schiller-University, Erbertstr. 1, 07743 Jena, Germany

e-mail: paul.lukas@uni-jena.de

Manuscript received: 29 January 2021

Accepted: 16 April 2021 by JÖRN KÖHLER

Abstract. *Alytes muletensis* is a frog endemic to the Balearic island of Majorca (or Mallorca). Its tadpole lives in semi-permanent plunge pools which remain after mountain streams have dried up. Little is known about the morphology of the different members of the Alytidae and the relationships of its members are still unclear. Alytidae are among the most basal anurans, and improved knowledge of their larval morphology can contribute to our understanding of the morphological evolution of anurans. Herein, I describe the external morphology as well as skeletal and muscular features of a tadpole of *A. muletensis* at GOSNER stage 25 by using standard histology, clearing and staining and 3D-reconstruction based on serial sections. The tadpole displays different discoglossoid traits such as the presence of two portions of the *M. levator mandibulae externus*, the separation of hypobranchial elements by the basibranchial, and the absence of the *M. constrictor branchialis IV*, among others. Unusual is the absence of the *M. constrictor branchialis I* as well as the absence of the *M. intermandibularis*. Remarkable is the presence of the admandibular cartilage as an additional skeletal element of the lower jaw.

Key words. Amphibia, Anura, Alytidae, Discoglossoidea, Ferreret, admandibular cartilage.

Introduction

Alytes muletensis (SANCHIZ & ADROVER, 1979), the Ferreret or Majorcan midwife toad, is a small anuran species endemic to the Balearic island of Majorca (aka. Mallorca). In 1977 it was thought to be extinct and therefore described from fossil remains as *Baleaphryne muletensis* (SANCHIZ & ADROVER, 1979). Its rediscovery in six isolated streams within barely accessible gorges of the Serra de Tramuntana in 1980 was nothing less than a herpetological sensation (MAYOL et al. 1980, MAYOL & ALCOVER 1981). The formerly widespread species was expelled from its original habitats by competitors and predators such as *Pelophylax perezi* (LÓPEZ SEOANE, 1885) and *Natrix maura* (LINNAEUS, 1758) brought in by the Romans about 2000 years ago (BUSH 1994). Its low abundance led to the initiation of numerous captive breeding programs (TONGE & BLOXAM 1991, BULEY & GARCIA 1997). Population reinforcement measures were a success and led to increasing numbers of both adults and larvae (VALLS et al. 2014). *Alytes muletensis* is one of the few examples in which the conservation status of a species has improved from “critically endangered” to “vulnerable” (SERRA et al. 2009).

The Majorcan midwife toad lives in mountainous regions in the northeast of the island. Its habitat is restricted to deep and barely accessible limestone gorges due to pressures exerted by introduced competitors and predators.

Adults live in cracks on the cliff faces, whereas the tadpoles are deposited in semi-permanent plunge pools, which remain after mountain streams have dried up (BUSH & BELL 1997, TONGE & BLOXAM 1989). Breeding mostly takes place in May and June. *Alytes muletensis* displays a special breeding behaviour where the male wraps a string of 9–24 eggs around his hind limbs after they are laid. He carries, protects and moistens the clutch until the offspring is close to hatching. Then the male releases the tadpoles in shallow water, where they will develop until metamorphosis (BUSH 1996, TONGE & BLOXAM 1989). The adults have a large head and relatively long fingers and toes. The eyes are large and have a vertical slit-shaped pupil. The coloration is very variable, ranging from a brownish to greenish background and a pattern of green to black spots. Every individual has its own unique pattern (VITT & CALDWELL 2009, HALLIDAY 2016). Females (38 mm) are slightly larger than males (35 mm) but there is no obvious sexual dimorphism (TONGE & BLOXAM 1989). The tadpoles (Fig. 1) are dark and slender and can grow to a total length of 76 mm (MAYOL & ALCOVER 1981, AmphibiaWeb 2021).

Frogs of the family Alytidae are represented by twelve species in three genera, including *Alytes* (6 species), *Discoglossus* (5 species), and the recently rediscovered *Latonia* (BITON et al. 2013). Together with the Bombinatoridae they belong to the Discoglossoidea and are after the Leiolelmatodea the second branch within the anuran clade

(PYRON & WIENS 2011, FENG et al. 2017). The 6 species of *Alytes* are widely distributed within western Europe and Morocco. The exact phylogenetic relationships of the different species and subgenera in the genus *Alytes* have been subjects of several investigations (GONÇALVES et al. 2007, MAIA-CARVALHO et al. 2014, DUFRESNES & MARTÍNEZ-SOLANO 2020), which recovered *A. muletensis* as sister taxon to *A. dickhilleni* (ARNTZEN & GARCÍA-PARÍS, 1995) and *A. maurus* (PASTEUR & BONS, 1962).

Little is known about the musculoskeletal features of larval *A. muletensis*. This work therefore provides a comprehensive description of its larval musculoskeletal morphology. It adds important larval morphological data of a member of Alytidae to the scientific record for future use in works focussing on the musculoskeletal features of larval anurans. The described features are also discussed in a phylogenetic context and compared to closely related anurans.

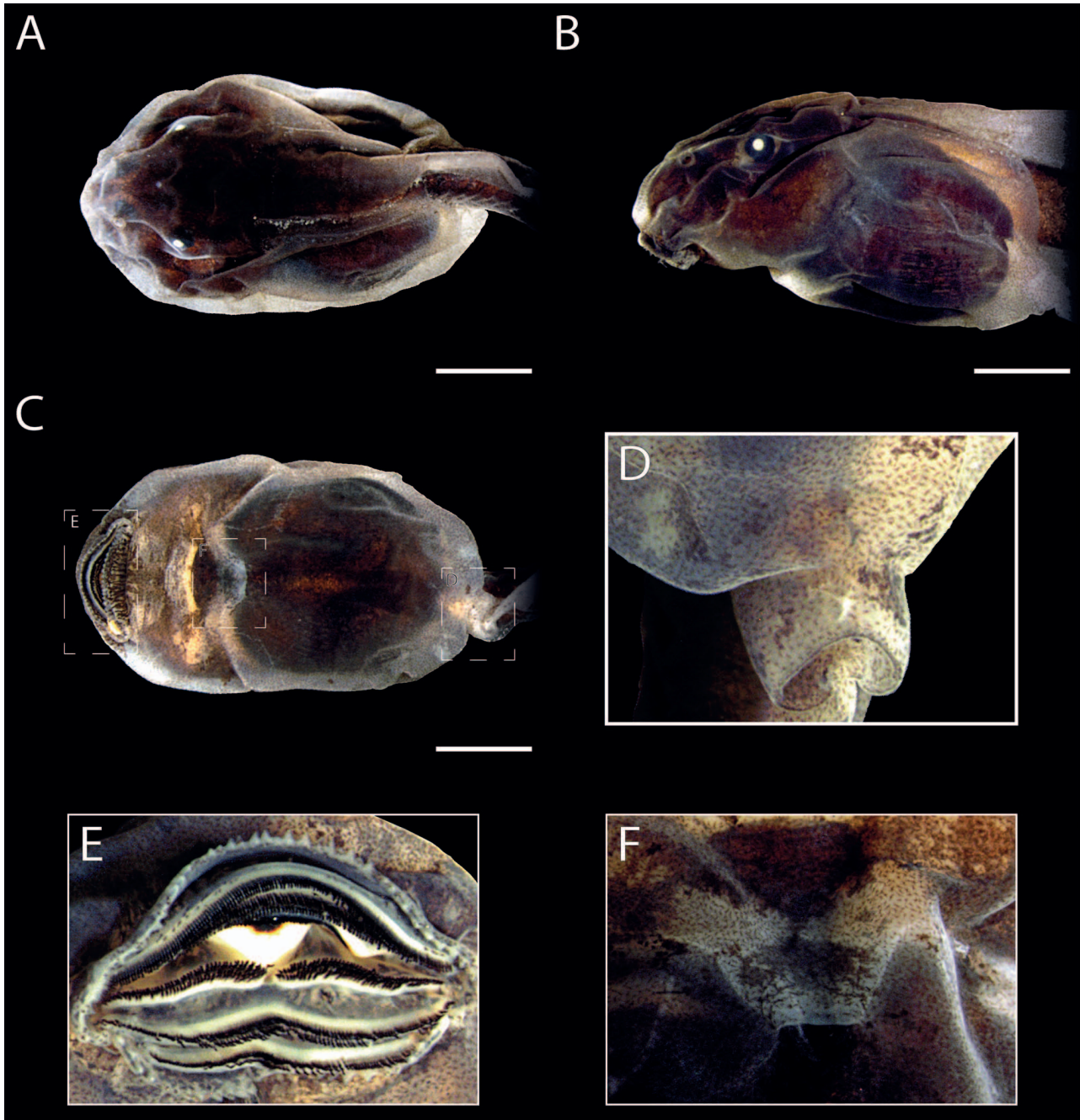


Figure 1. Tadpole of *Alytes muletensis* in (a) dorsal, (b) lateral and (c) ventral views. Detailed views of the (d) vent tube, (e) oral disc and (f) spiracle. Scale bars equal 2 mm.

Materials and methods

The ten specimens of *A. muletensis* used in this study were provided by a private breeder. They were part of different clutches, had died of natural causes during development, and were fixed in 4% phosphate-buffered formalin (PFA) for one week and transferred to 70% ethanol for long-term storage at 23°C. They were staged according to GOSNER (1960) and measured as specified by ALTIG (2007). Terminology used for descriptions follow the guidelines introduced by HAAS (2003) for musculoskeletal features. Measurements were taken using an ocular micrometer mounted on a Zeiss STEMI SV11. Four tadpoles were dehydrated, embedded in paraffin, and serially sectioned at 7 µm using a rotary microtome (Microm, HM 355 S). The transversally orientated serial sections were collected on a microscope slide and stained according to Heidenhain's Azan technique (HEIDENHAIN 1915). Slides were digitized using a Axio Scan Z1 operated with Zen 3.1. Four tadpoles were cleared and stained in whole-mount following a standard protocol (DINGERKUS & UHLER 1977). They were examined and photographed using a Zeiss STEMI SV11 and an attached camera (ColorView) operated by ANALYSIS software. Dissected larvae (2 specimens), cleared-and-stained larvae (4 specimens), and histological slides (4 series) are stored at the Institute of Zoology and Evolutionary Research, Friedrich-Schiller-University, Jena.

The digitized slide images were exported to Fiji Software (SCHINDELIN et al. 2012). They were stacked and aligned using first the least squares (rigid) and second the elastic non-linear block correspondence mode from the TrakEM2 plugin for Fiji (CARDONA et al. 2012). Elastically aligned stacks were exported as tagged image files (TIFF). Segmentation of the different musculoskeletal structures was performed in Amira 6.0.1. 3D analysis software (FEI Visualization Sciences Group). Polygonal surfaces were rendered and then exported to Wavefront OBJ file format for further processing in Autodesk Maya 2020 (Autodesk, Inc.). Surfaces were smoothed, polygonal counts reduced, and the surfaces arranged. For the final composition and rendering of images, Autodesk Mudbox 2020 (Autodesk, Inc.) was used. All images were edited and arranged using Adobe Photoshop CS6 and Adobe Illustrator CS6 (Adobe Inc.). The following results are based on tadpoles at GOSNER stage 25 (Go25).

Results

Cranial skeleton

The chondrocranium of *A. muletensis* is well chondrified at Go25. It is almost as long as wide and dorsoventrally depressed. The highest width is at the level of the posterior subocular bar. The suprarostal cartilage is the most anterior cartilaginous part of the skeleton (Figs 2B, 3A). It is a single cartilage which is jointed synchondrotically at its two medial processes with the paired trabecular horns. The alae are laterally situated, plate-like in shape, and bear a

well-developed dorsal anterior and a less conspicuous dorsal posterior process. The suprarostal corpus is U-shaped with a small median band connecting both halves.

The U-shaped ventral margin of the suprarostal cartilage surrounds the infrarostal cartilage anteriorly (Fig. 2B). The infrarostal cartilage is a paired cartilage (Figs 3B, C). It is a broad, slightly diagonally orientated paired cartilage. The mediolateral surface of each infrarostal cartilage is connected to the rounded anterior tip of each Meckel's cartilage via the intramandibular joint.

Meckel's cartilage is a paired and sigmoid cartilage between the infrarostal cartilage and the palatoquadrate (Fig. 2B). The medial surface is straight, whereas the lateral surface is typically curved. Posteriorly it bears a well-developed retroarticular process which surrounds the articular process of the palatoquadrate ventrally (Figs 2C, 3D). In between is situated a hinge-like jaw joint. Lateral to the anterior part of Meckel's cartilage a paired admandibular cartilage is present. It is a small, dorsoventrally projecting cartilaginous rod (Fig. 3C).

The palatoquadrate is a broad, plate-like cartilage on the lateral margin of the cranial skeleton. It is anchored to the neurocranium via the anterior quadratocranial commissure and the posterior ascending process. The third neurocranial anchoring process, the larval otic process, is absent or not yet developed in the investigated specimens. The articular process on the anterior edge of the palatoquadrate is broad and has a lateral projection which proceeds anteriorly around the lateral edge of Meckel's cartilage. Medially, the ethmoid process, directed anteriorly, is present (Fig. 2A). The muscular process is very high and almost reaches the height of the lateral brain wall (Fig. 2C). The quadratocranial commissure is broad with an antorbital process on its anterior margin. The oval subocular fenestra is bordered laterally by a broad subocular bar, which is plane anteriorly but bends vertically on its posterior surface, which results in a bulging posterior margin. The ascending process is a thick rod which proceeds dorsally at an angle of 45°.

The trabecular horns are jointed synchondrotically anteriorly to the suprarostal cartilage. The two cartilaginous bars proceed vertically. Where they reach the plane of the dorsal tip of the muscular process, they bend at a right angle and proceed horizontally in posterior direction. They unite and form a short ethmoid plate (Fig. 3D). On its lateral wall the orbitonasal foramen is present. Posteriorly, the high marginal tectal taeniae arise from the lateral surface of the ethmoid plate (Fig. 2A). They border the frontoparietal fenestra. At the centre of the lateral brain wall, a small triangular projection proceeds medially, which may be a very short transversal tectal taenia (Fig. 2A). A small basicranial fenestra is present in the cranial floor. The lateral wall of the braincase bears three foramina. Medially, a circular optic foramen is present. Ventral to the insertion of the ascending process on the lateral wall of the braincase, there is a small trochlear foramen, which is dorsal to the largest foramen, the oculomotor foramen. The otic capsules reach about 30% of the

The basibranchial resembles the shape of a kite square (Fig. 2B). Its anterior part separates the two parts of the ceratohyal, whereas its posterior part separates the hypobranchial elements. Medioventrally it bears a rounded but not prolonged urobranchial process. Its lateral surface is

connected to the hypobranchial plate and the ceratohyal by chondroid tissue.

The branchial basket consists of a flat hyobranchial plate which is broader anteriorly than posteriorly. The hyobranchial plate is connected synchondrotically to the

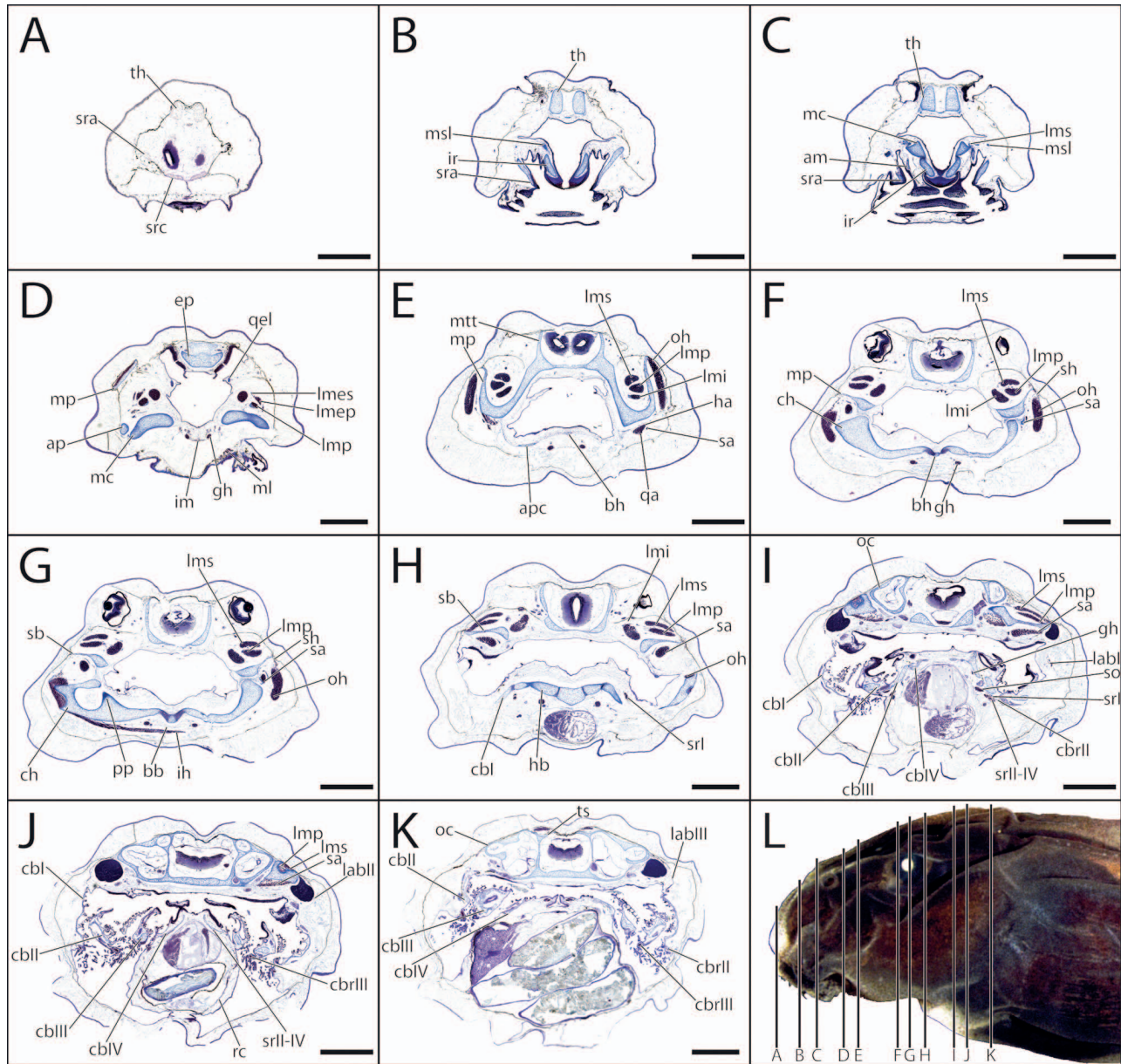


Figure 3. Transverse sections through a tadpole of *Alytes muletensis*, Go 25. (a–k) sections at different planes as indicated in (l). Scale bars equal 1 mm. am, admandibular cartilage; apc, anterior process of ceratohyal; bb, basibranchial; bh, basihyal; cbl–IV, ceratobranchial I–IV; cbrII+III, M. constrictor branchialis II+III; ch, ceratohyal; ep, ethmoid plate; gh, M. geniohyoideus; ha, M. hyoangularis; ich, M. interhyoideus; hb, hypobranchial plate; im, M. intermandibularis; ir, infrarostral cartilage; labI–III, M. levator arcuum branchialium I–III; lmp, M. levator mandibulae longus superficialis; lms, M. levator mandibulae longus superficialis; mc, Meckel's cartilage; ml, M. mandibulolabialis; mp, muscular process; mtt, marginal tectal taenia; oc, otic capsule; oh, M. orbitohyoideus; pp, processus postcondylaris; qa, M. quadratoangularis; qel, quadratoethmoid ligament; rc, M. rectus cervicis; sa, M. suspensorioangularis; sb, subocular bar; sh, M. suspensoriohyoideus; so, M. subarcualis obliquus; sra, suprarrostral ala; src, suprarrostral corpus; srl, M. subarcualis rectus I; srlII–IV, M. subarcualis rectus II–IV; th, trabecular horn; ts, tectum synoticum.

rest of the branchial basket at two points, near the proximal parts of ceratobranchials II and III. All four ceratobranchials are present and proceed diagonally (Fig. 2B). They are fused caudally via the terminal commissures I–III and rostrally via the proximal commissures I–III. Ceratobranchial I bears two lateral projections and an anterior branchial process. Ceratobranchials II and III each possess a small branchial process proximally. Spicules II and III are conspicuous and elongated. Spicule II originates from the proximal part of ceratobranchial II and proceeds rostrally, whereas spicule III originates from the proximal part of ceratobranchial III and proceeds caudally.

Ligaments

The investigated tadpoles of *A. muletensis* have three mandibular ligaments. The suprarostrals-quadrates ligament originates from the anterior tip of the articular process of the palatoquadrate. It proceeds in anterodorsal direction and inserts at the dorsomedian surface of the suprarostrals ala (Fig. 2C). Another ligament that inserts on the suprarostrals ala is the mandibulo-suprarostrals ligament. It originates from the anteromedian tip of Meckel's cartilage in close proximity to the insertion of the *M. levator mandibulae externus superficialis*. It inserts on the postero-dorsal surface of the suprarostrals ala, posterior to the insertion of the suprarostrals-quadrates ligament (Fig. 2C). The quadratoethmoid ligament is the longest ligament and spans between the quadratoethmoid process and the mediolateral surface of the trabecular horn (Figs 2C, 3D).

Muscles

An overview of the origin and insertion of each observed muscle is given in Table 1. The investigated larvae of *A. muletensis* lack the *M. intermandibularis anterior*, *M. levator mandibulae lateralis*, *M. interhyoideus posterior*, the *M. constrictor branchialis I*, the *M. constrictor branchialis IV*, the *M. tympanopharyngeus*, *M. diaphragmatobranchialis*, and the *M. transversus ventralis IV*, or they are not developed yet or fused to another muscle and therefore not observable.

The typical six extrinsic eye muscles are present in *A. muletensis*. It is notable that the *M. obliquus superior* and the *M. obliquus inferior* have the same origin on the anterolateral surface of the marginal tectal taenia. The *M. obliquus inferior* and the *M. rectus posterior* are in close proximity at their insertion on the bulbus oculi (Fig. 2C).

The *M. levator mandibulae longus superficialis* spans over all other levator muscles dorsally and inserts close to the *M. levator mandibulae externus superficialis* (Fig. 2A). The insertion of the latter is in close proximity to the mandibulo-suprarostrals ligament and some fibres of this muscle are attached to it. The *M. levator mandibulae longus profundus* and *M. levator mandibulae internus* both end in a long tendon and insert on the suprarostrals ala and Meckel's

cartilage, respectively. The *M. levator mandibulae externus profundus*, the second portion of the *M. levator mandibulae externus* present in *A. muletensis*, shares its insertion on the suprarostrals ala with the *M. levator mandibulae longus profundus*. The *M. levator mandibulae articularis* is the shortest jaw levator (Fig. 2C). The *M. mandibulolabialis* is a fan-shaped muscle whose fibres spread to all tooth rows of the lower lip (Fig. 2B).

The *M. intermandibularis posterior* is a dorsoventrally depressed (Fig. 3D), flat muscle that extends far caudally. Its posterior fibres are close to the medioanterior margin of the *M. interhyoideus* (Fig. 2B). Noteworthy is the presence of the *M. suspensoriohyoideus*, proceeding from the posterodorsal margin of the muscular process to the lateral process of the ceratohyal (Figs 2C, 3F). The *M. orbitohyoideus* covers most of the muscular process (Fig. 3E) and surrounds the lateral process of the ceratohyal laterally, dorsally and medially (Figs 2C, 3H). The *M. quadratoangularis*, *M. hyoangularis* and *M. suspensorioangularis* proceed parallel to each other. The latter is the longest jaw depressor and originates far caudally in the suborbital area of the palatoquadrate (Fig. 3J).

All four branchial basket levators are well developed. *M. levatores arcuum branchialium I–II* are wide and the *M. levatores arcuum branchialium* more narrow muscles (Fig. 2C). A wide gap is present between *M. levator arcuum branchialium I* and *II*, whereas the *M. levatores arcuum branchialium II–IV* are each separated by a narrow gap. The *M. constrictor branchialis II* and *III* span over their respective ceratobranchial in an arch-like manner (Fig. 2B). The *M. subarcualis obliquus* has a broad origin from the branchial process *II* and *III* proceeds obliquely and inserts on the median urobranchial process (Figs 2B, 3I). The *M. subarcualis rectus I* has two caudal slips, which originate at the proximal ceratobranchial *I* (dorsal slip) and the anterior surface of ceratobranchial *II* (ventral slip). It connects the branchial basket with the caudal margin of the ceratohyal. The *M. subarcualis rectus II–IV* are the ventralmost of the branchial muscles, connecting the proximal surfaces of ceratobranchial *I* and ceratobranchial *IV* (Fig. 2B).

Discussion Morphology

Most of the skeletal features of *A. muletensis* resemble the description of *A. obstetricans* (LAURENTI, 1768) even though no pseudopterygoid process is present in *A. muletensis* (VAN SETERS 1922). The suprarostrals cartilage is synchondrotically connected to the trabecular horns at the two dorsal projections of the suprarostrals corpus. This condition is similar to others described from *Discoglossoida* (PÜGENER & MAGLIA 1997, HAAS 2001, LUKAS & OLSSON 2020). In the more basal frog *Ascaphus truei* (STEJNEGER, 1899) the suprarostrals cartilage is solidly connected to the neurocranium (PUSEY 1943, REISS 1997). Therefore, the synchondrotic condition in *Discoglossoids* may re-

Table 1. Overview of the larval cranial musculature of *Alytes muletensis*, Go25.

Muscle	Origin	Insertion	Comments
Eye muscles			
Obliquus inferior	anterior surface of marginal tectal taenia	medioventral bulbus oculi	shares origin with M. obliquus superior
Obliquus superior	anterior surface of marginal tectal taenia	anterodorsal bulbus oculi	shares origin with M. obliquus inferior
Rectus anterior	anterior margin of oculomotor foramen	anteromedial bulbus oculi	
Rectus posterior	medioventral margin of oculomotor foramen	medioventral bulbus oculi	
Rectus inferior	dorsal margin of oculomotor foramen	caudomedial bulbus oculi	
Rectus superior	caudal margin of oculomotor foramen	caudodorsal bulbus oculi	
Mandibular arch muscles			
Lev. mand. longus superficialis	laterocaudal surface of the subocular cartilage	anterodorsal tip of Meckel's cartilage	
Lev. mand. longus profundus	dorsocaudal surface of the subocular cartilage	caudoventral surface of suprarostrale ala	ends in a long tendon
Lev. mand. internus	ventral surface of ascending process	dorsolateral surface of Meckel's cartilage	ends in a long tendon
Lev. mand. externus superficialis	medial, inferior surface of muscular process (superior)	anterodorsal tip of Meckel's cartilage	insertion close to mandibulo-suprarostrale ligament
Lev. mand. externus profundus	medial, inferior surface of muscular process (medial)	caudoventral surface of suprarostrale ala	shares tendon with M. l. m. l. profundus
Lev. mand. articularis	medial, inferior surface of muscular process (inferior)	dorsomedial surface of Meckel's cartilage	
Mandibulolabialis	caudomedian surface of Meckel's cartilage	lower lip	fans out to all posterior tooth rows
Hyoid arch muscles			
Hyoangularis	lateral surface of the anterolateral process of ceratohyal	posterior tip of the retroarticular process of Meckel's cartilage lateral to the insertion of the M. quadratoangularis	
Quadratoangularis	ventral anterior surface of palatoquadrate	posteromedial surface of the retroarticular process of Meckel's cartilage	
Suspensorioangularis	caudoventral surface of subocular cartilage	lateral surface of retroarticular process of Meckel's cartilage	
Orbitohyoideus	lateral surface of muscular process	anterior surface of lateral process of ceratohyal	
Suspensoriohyoideus	caudolateral surface of muscular process	dorsal tip of lateral process of ceratohyal	
Intermandibularis posterior	caudomedial surface of Meckel's cartilage, median to origin of M. mandibulolabialis	median raphe	posterior fibers adjacent to anterior part of M. interhyoideus
Interhyoideus	ventrolateral surface of ceratohyal	median raphe	
Branchial arch muscles			
L. arc. branchialium I	ventrolateral surface of subocular cartilage	lateral projection of cbI	
L. arc. branchialium II	caudal surface of subocular cartilage, lateral margin of otic capsule	terminal commissure I	
L. arc. branchialium III	lateral margin of otic capsule, caudal to M. l. arc. branchialium II	caudolateral process of cbII	
Lev. arc. branchialium IV	caudolateral margin of otic capsule	caudal surface of cbIV	

Table 1 continued

Muscle	Origin	Insertion	Comments
Constr. branchialis II	terminal commissure I	anteromedial part of ceratobranchial II	
Constr. branchialis III	terminal commissure II	caudomedial part of ceratobranchial II	
Subarcualis rectus I	dorsal head proximal ceratobranchial I, ventral head anterior surface of ceratobranchial II	caudal surface of ceratohyal, lateral to posterior process	
Subarcualis rectus II-IV	rostroventral surface of ceratobranchial IV	rostroventral surface of ceratobranchial I	
Subarcualis obliquus II	branchial process II + III	urobranchial process of basibranchial	
Hypobranchial muscles			
Geniohyoideus	anteromedial surface of ceratobranchial III	caudolateral surface of infrastral cartilage	
Rectus cervicis	peritoneum	medial surface of ceratobranchial III	

flect the evolutionary trend from a solid connection, via a synchondrotic connection, towards a free and movable suprarostal cartilage in more derived anurans. The infrastral cartilage is paired as described for *A. obstetricans* (VAN SETERS 1922) but differs from the unpaired infrastral cartilage in *A. obstetricans* depicted by HAAS (2001). An intramandibular commissure between Meckel's cartilage and infrastral cartilage was not observed in *A. muletensis* in contrast to *A. obstetricans* (HAAS 2001). The admandibular cartilage is a vertically orientated rod without any muscular connection and is similar in condition to that described from *A. obstetricans* (HAAS 2003). It is also present in species of *Discoglossus* and *Heleophryne* (VAN SETERS 1922, VAN DER WESTHUIZEN 1961, PÚGENER & MAGLIA 1997, KRÁLOVEC et al. 2010, LUKAS 2020) but not in *Bombina orientalis* (BOULENGER, 1890). Its function as well as its evolutionary origin remain debatable (LUKAS & OLSSON 2018a, LUKAS 2020). In *A. muletensis* the dorsal tip of this cartilage is bordered by the mandibulo-suprarostal ligament. It seems possible that the tightening of this ligament during jaw opening pushes the admandibular cartilage in a ventral direction where it is pushed rostrally by Meckel's cartilage. This may induce a spatial proximity to the M. mandibulolabialis, thus the movement of the admandibular cartilage may refine muscle activity or limit the movement of Meckel's cartilage and therefore refine jaw function. Otherwise, it was proposed that the admandibular cartilages evolved as part of oral adhesive mechanisms (SOKOL 1981). Meckel's cartilage, the palatoquadrate, and neurocranial structures of *A. muletensis* mostly resemble the features described from other Discoglossidae (VAN SETERS 1922, PUGENER et al. 2003, LUKAS & OLSSON 2020). Remarkable is the nearly 45°-angle of the palatoquadrate in lateral view, proceeding from rostral to caudal and the bulging posterior margin, which is also present in *Discoglossus sardus* (TSCHUDI, 1837) and *B. orientalis* (PÚGENER & MAGLIA 1997, LUKAS & OLSSON 2020). The processus postcondylaris is a small and triangular process on the

dorsoposterior face of the ceratohyal. It is present in several species of *Ascaphus*, *Alytes*, *Bombina* and *Discoglossus* (HAAS 1997, 2003). In *A. muletensis* the basibranchial separates the ceratohyal and hypobranchial elements medially. At least the separation of the hypobranchial elements may be conserved in members of the Discoglossidae (HAAS 1997), which delimits the Discoglossidae from the Pipanura where the hypobranchial elements of species such as *Xenopus laevis* (DAUDIN, 1802) are medially fused (LUKAS & OLSSON 2018b). The branchial basket of *A. muletensis* bears some features which are shared with its close relatives. The spicules II and III are elongated as described for *A. obstetricans* (HAAS 2003) and *D. sardus* (PÚGENER & MAGLIA 1997), and they are present but tiny in *Discoglossus pictus* (OTTH, 1837) and *Discoglossus galganoi* (CAPULA, NASCETTI, LANZA, BULLINI & CRESPO, 1985) (HAAS 2003). The complete absence of spicules in *Bombina variegata* (LINNAEUS, 1758) and *B. orientalis* (HAAS 2003, LUKAS & OLSSON 2020) may be a supportive character for the close relationship of Alytinae and Discoglossinae.

The musculature of *A. muletensis* larvae shows many similarities to the closely related species *A. obstetricans*, but *A. muletensis* lacks a M. intermandibularis anterior, which is present in *A. obstetricans* and *B. orientalis* (HAAS 2001, OLSSON et al. 2001). The mandibular ligaments and the mandibular arch derived musculature of *A. muletensis* are similar to the condition described from *A. obstetricans* (HAAS 2001). In both investigated *Alytes* species, as well as in *B. orientalis*, the M. levator mandibulae lateralis is absent (HAAS 2001, OLSSON et al. 2001). This muscle is also absent in pipids (ZIERMANN & OLSSON 2007). The M. levator mandibulae lateralis arises in more derived anurans and is a defining feature of the pelobatoid and neobatrachian clades (HAAS 2003). The M. intermandibularis of *A. muletensis* is V-shaped and flat. It originates on the caudomedial surface of Meckel's cartilage in close proximity to the origin of the M. mandibulolabialis. Its posterior face is bordered by the anterior face of M. interhyoideus. This condi-

tion is also present in *A. truei*, *A. obstetricans*, *B. maxima*, and *D. galganoi* (SCHOLSSER & ROTH 1995, HAAS 2001, 2003) and supports their close relationships. The *M. suspensorioangularis* originates far posteriorly in species of *Ascaphus*, *Alytes*, *Bombina*, *Discoglossus* and *Heleophryne* (HAAS 2003, LUKAS 2020), and it may resemble the condition of the *M. depressor mandibulae* found in salamanders (HAAS 1997). It is missing in *Pipa* and *Xenopus* (SOKOL 1977, ZIERMANN & OLSSON 2007), which is considered a secondary loss and not a synapomorphic character for all pipanurans. The *Mm. levatores arcuum branchialium* I and II are separated by a wide gap, as has been described for other Discoglossoidea and also Heleophrynids (HAAS 1997, 2003, LUKAS 2020). Some unique conditions are found in the branchial musculature. No *M. constrictor branchialis* I is present, as in other Discoglossoidea investigated so far (HAAS 1997). The remaining branchial muscles are similar to what has been described from *A. obstetricans* (HAAS 1997). Remarkable is the origin of the *M. subarcualis rectus* I at the ceratobranchials I and II, as well as the origin of the *M. subarcualis obliquus* at the branchial processes II and III. This is a unique condition found in no other anuran larvae so far.

Systematics

Based on the described characters of *A. muletensis* and recent investigations in various closely related taxa, this work supports several apomorphic characters for different basal anuran clades. The processus postcondylaris of the ceratohyal is present in most of the Leiopelmatoidea, except in *Leiopelma* species (STEPHENSON 1951), as well as in all Discoglossoidea investigated so far (HAAS 1997, 2003). Another feature, which is present in the given basal taxa, is the V-shaped *M. intermandibularis posterior*, whose posterior surface lies in close proximity to the anterior margin of *M. interhyoideus*. (1) The presence of the processus postcondylaris and (2) the specific shape and dimension of the *M. intermandibularis posterior*, as well as (3) the absence of the *M. levator mandibulae lateralis* may be synapomorphic characters for all anurans.

Several characters are present that underline the monophyletic state of the Discoglossoidea (HAAS 1997, 2003). They are supported by the observations of the present work. Traits of the Discoglossoidea are therefore the (1) bulging posterior margin of the palatoquadrate, (2) the two portions of the *M. levator mandibulae externus*, (3) the separation of hypobranchial elements by the posterior projection of the basibranchial, (4) the origination of the *M. geniohyoideus* for ceratobranchial III, and (5) the absence of a *M. constrictor branchialis* IV.

The relationships of the families within the Discoglossoidea are discussed in many morphological and molecular cladistic investigations (HAAS 2003, SAN MAURO et al. 2005, FROST et al. 2006, PYRON & WIENS 2011, FENG et al. 2017). Based on the description of larval features of *A. muletensis* and recent works on species of *Bombina* and *Disco-*

glossus, supportive features for Alytidae, comprising of Alytinae and Discoglossinae, are the (1) presence of spicules II and III, and (2) the presence of admandibular cartilages.

Defining features of the genus *Alytes* are supposed to be the (1) origin of the *M. subarcualis obliquus* at ceratobranchials II and III, and the (2) origin of the *M. subarcualis rectus* I at ceratobranchials I and II. The absence of the *M. constrictor branchialis* I as well as the absence of the *M. intermandibularis anterior* is unique to *A. muletensis*.

Conclusion

This study presents a comprehensive description of the understudied larva of *A. muletensis*, which is part of the second basal branch of all anurans. Especially the recently described unique configuration of several branchial muscles in the close relative, *A. obstetricans* (HAAS 1997), was confirmed in this study. Furthermore, various morphological features delimit *A. muletensis* from its closest relatives. Important morphological features and potential synapomorphies of the Discoglossoidea are added to the record and set the baseline for further investigations on larval morphology of closely related taxa as well as for further research on anuran evolution and systematics. Larval anurans are less studied than their respective adults despite bearing many adaptations and unique features that are needed to fully understand the evolution of this diverse group.

Acknowledgements

The present study was funded by a grant from the Deutsche Forschungsgemeinschaft (grant no. LU 2404/1-1). I am very grateful to KATJA FELBEL for technical support and preparation of the histological sections and to the two anonymous breeders who provided valuable information on the biology of *Alytes muletensis*.

References

- ALTIG, R. (2007): A primer for the morphology of anuran tadpoles. – *Herpetological Conservation and Biology*, **2**: 71–74.
- AmphibiaWeb (2021): *Alytes muletensis*: Mallorcan Midwife Toad. – University of California, Berkeley, CA, USA. <https://amphibiaweb.org/species/1521>, accessed 13 April 2021.
- BITON, R., E. GEFFEN, M. VENCES, O. COHEN, S. BAILON, R. RABINOVICH, Y. MALKA, T. ORON, R. BOISTEL, V. BRUMFELD & S. GAFNY (2013): The rediscovered Hula painted frog is a living fossil. – *Nature Communications*, **4**: 1959.
- BULEY, K. R. & G. GARCIA (1997): The recovery programme for the Mallorcan midwife toad *Alytes muletensis*: an update. – *Dodo-Journal of the Wildlife Preservation Trusts*, **33**: 80–90.
- BUSH, S. (1994): Good news for the Majorcan midwife toad. – *Froglog (IUCN/SSC Declining Amphibian Populations Task Force Newsletter)*, **1**.
- BUSH, S. & D. J. BELL (1997): Courtship and female competition in the majorcan midwife toad, *Alytes muletensis*. – *Ethology*, **103**: 292–303.

- BUSH, S. L. (1996): Why is double clutching rare in the Majorcan midwife toad? – *Animal Behaviour*, **52**: 913–922.
- CARDONA, A., S. SAALFELD, J. SCHINDELIN, I. ARGANDA-CARRERAS, S. PREIBISCH, M. LONGAIR, P. TOMANCAK, V. HARTENSTEIN & R. J. DOUGLAS (2012): TrakEM2 software for neural circuit reconstruction. – *PLoS One*, **7**: 38011–38011.
- DINGERKUS, G. & L. D. UHLER (1977): Enzyme clearing of alcian blue stained whole small vertebrates for demonstration of cartilage. – *Stain Technology*, **52**: 229–32.
- DUFRESNES, C. & Í. MARTÍNEZ-SOLANO (2020): Hybrid zone genomics supports candidate species in Iberian *Alytes obstetricans*. – *Amphibia-Reptilia*, **41**: 105–112.
- FENG, Y. J., D. C. BLACKBURN, D. LIANG, D. M. HILLIS, D. B. WAKE, D. C. CANNATELLA & P. ZHANG (2017): Phylogenomics reveals rapid, simultaneous diversification of three major clades of Gondwanan frogs at the Cretaceous–Paleogene boundary. – *Proceedings of the National Academy of Sciences of the U.S.A.*, **114**: 5864–5870.
- FROST, D. R., T. GRANT, J. N. FAIVOVICH, R. H. BAIN, A. HAAS, C. LIO, F. B. HADDAD, R. O. DE, A. CHANNING, M. WILKINSON, S. C. DONNELLAN, C. J. RAXWORTHY, J. A. CAMPBELL, B. L. BLOTTO, P. MOLÉR, R. C. DREWES, R. A. NUSSBAUM, J. D. LYNCH, D. M. GREEN & W. C. WHEELER (2006): The amphibian tree of life. – *Bulletin of the American Museum of Natural History*, **297**: 1–291.
- GONÇALVES, H., I. MARTÍNEZ-SOLANO, N. FERRAND & M. GARCÍA-PARÍS (2007): Conflicting phylogenetic signal of nuclear vs mitochondrial DNA markers in midwife toads (Anura, Discoglossidae, *Alytes*): Deep coalescence or ancestral hybridization? – *Molecular Phylogenetics and Evolution*, **44**: 494–500.
- GOSNER, K. L. (1960): A simplified table for staging anuran embryos larvae with notes on identification. – *Herpetologica*, **16**: 183–190.
- HAAS, A. (1997): The larval hyobranchial apparatus of discoglossoid frogs: its structure and bearing on the systematics of the Anura (Amphibia: Anura). – *Journal of Zoological Systematics and Evolutionary Research*, **35**: 179–197.
- HAAS, A. (2001): Mandibular arch musculature of anuran tadpoles, with comments on homologies of amphibian jaw muscles. – *Journal of Morphology*, **247**: 1–33.
- HAAS, A. (2003): Phylogeny of frogs as inferred from primarily larval characters (Amphibia: Anura). – *Cladistics*, **19**: 23–89.
- HALLIDAY, T. (2016): The book of frogs: a life-size guide to six hundred species from around the world. – IVY Press, Brighton, 656 pp.
- HEIDENHAIN, M. (1915): Über die Mallorische Bindegewebsfärbung mit Karmin und Azokarmin als Vorfarben. – *Zeitschrift für wissenschaftliche Mikroskopie und mikroskopische Technik*, **33**: 361–372.
- KRÁLOVEC, K., Z. ROČEK, P. ŽÁKOVÁ & V. MUŽÁKOVÁ (2010): Development of the ethmoidal structures of the endocranium in *Discoglossus pictus* (Anura: Discoglossidae). – *Journal of Morphology*, **271**: 1078–1093.
- LUKAS, P. (2020): Larval cranial anatomy of the Eastern Ghost Frog (*Heleophryne orientalis*). – *Acta Zoologica* (early view).
- LUKAS, P. & L. OLSSON (2018a): Bapx1 upregulation is associated with ectopic mandibular cartilage development in amphibians. – *Zoological Letters*, **4**: 16.
- LUKAS, P. & L. OLSSON (2018b): Sequence and timing of early cranial skeletal development in *Xenopus laevis*. – *Journal of Morphology*, **279**: 62–74.
- LUKAS, P. & L. OLSSON (2020): Sequence of chondrocranial development in the oriental fire bellied toad *Bombina orientalis*. – *Journal of Morphology*, **281**: 688–701.
- MAIA-CARVALHO, B., H. GONÇALVES, N. FERRAND & I. MARTÍNEZ-SOLANO (2014): Multilocus assessment of phylogenetic relationships in *Alytes* (Anura, Alytidae). – *Molecular Phylogenetics and Evolution*, **79**: 270–278.
- MAYOL, J. & J.-A. ALCOVER (1981): Survival of *Baleaphryne Sanchíz* and Adrover, 1979 (Amphibia: Anura: Discoglossidae) on Mallorca. – *Amphibia-Reptilia*, **1**: 343–345.
- MAYOL, J., J.-A. ALCOVER, G. ALOMAR, G. POMAR, J. JURADO & D. JAUME (1980): Supervivència de '*Baleaphryne*' (Amphibia: Anura: Discoglossidae) a les muntanyes de Mallorca. Nota preliminar. – *Butlletí de la Institució Catalana d'Història Natural* Núm. 51, **45**: 115–119.
- MCDIARMID, R. W. & R. ALTIG (1999): Tadpoles: the biology of anuran larvae. – University of Chicago Press, Chicago and London, 444 pp.
- OLSSON, L., P. FALCK, K. LOPEZ, J. COBB & J. HANKEN (2001): Cranial neural crest cells contribute to connective tissue in cranial muscles in the anuran amphibian, *Bombina orientalis*. – *Developmental Biology*, **237**: 354–367.
- PUGENER, L. A., A. M. MAGLIA & L. TRUEB (2003): Revisiting the contribution of larval characters to an analysis of phylogenetic relationships of basal anurans. – *Zoological Journal of the Linnean Society* **139**: 129–155.
- PUGENER, L. A. & A. M. MAGLIA (1997): Osteology and skeletal development of *Discoglossus sardus* (Anura: Discoglossidae). – *Journal of Morphology*, **233**: 267–286.
- PUSEY, H. K. (1943): On the head of the liopelmid frog, *Ascaphus truei*. – *Journal of Cell Science*, **82-84**: 105–185.
- PYRON, R. A. & J. J. WIENS (2011): A large-scale phylogeny of Amphibia including over 2800 species, and a revised classification of extant frogs, salamanders, and caecilians. – *Molecular Phylogenetics and Evolution*, **61**: 543–583.
- REISS, J. O. (1997): Early development of chondrocranium in the tailed frog *Ascaphus truei* (Amphibia: Anura): implications for anuran palatoquadrate homologies. – *Journal of Morphology*, **231**: 63–100.
- SAN MAURO, D., M. VENCES, M. ALCOBENDAS, R. ZARDOYA & A. MEYER (2005): Initial diversification of living amphibians predated the breakup of Pangaea. – *American Naturalist*, **165**: 590–599.
- SANCHÍZ, B. & R. ADROVER (1979): Anfíbios fósiles del Pleistoceno de Mallorca. – *Doñana Acta Vertebrata*, **4**: 5–25.
- SCHINDELIN, J., I. ARGANDA-CARRERAS, E. FRISE, V. KAYNIG, M. LONGAIR, T. PIETZSCH, S. PREIBISCH, C. RUEDEN, S. SAALFELD, B. SCHMID, J.-Y. TINEVEZ, D. J. WHITE, V. HARTENSTEIN, K. ELICEIRI, P. TOMANCAK & A. CARDONA (2012): Fiji: an open-source platform for biological-image analysis. – *Nature Methods*, **9**: 676–682.
- SCHOLSSER, G. & G. ROTH (1995): Distribution of cranial and rostral spinal nerves in tadpoles of the frog *Discoglossus pictus* (Discoglossidae). – *Journal of Morphology*, **226**: 189–212.
- SERRA, J. M., R. GRIFFITHS, J. BOSCH, T. BEEBEE, B. SCHMIDT, M. TEJEDO, M. LIZANA, I. MARTÍNEZ-SOLANO, A. SALVADOR, M.

- GARCÍA-PARÍS, E. R. GIL & J. W. ARNTZEN (2009): *Alytes muletensis*. – The IUCN Red List of Threatened Species.
- VAN SETERS, W. H. (1922): Le développement du chondrocrâne d'*Alytes obstetricans* avant la métamorphose. – Archives de Biologie, **32**: 373–491.
- SOKOL, O. M. (1977): The free swimming *Pipa* larvae, with a review of pipid larvae and pipid phylogeny (Anura: Pipidae). – Journal of Morphology, **154**: 357–425.
- SOKOL, O. M. (1981): The larval chondrocranium of *Pelodytes punctatus*, with a review of tadpole chondrocrania. – Journal of Morphology, **169**: 161–183.
- STEPHENSON, N. G. (1951): On the development of the chondrocranium and visceral arches of *Leiopelma archeyi*. – Transactions of the Zoological Society of London, **27**: 203–253.
- TONGE, S. J. & Q. M. C. BLOXAM (1989): Breeding the Mallorcan midwife toad *Alytes muletensis* in captivity. – International Zoo Yearbook, **28**: 45–53.
- TONGE, S. J. & Q. M. C. BLOXAM (1991): The breeding programme for the Mallorcan midwife toad *Alytes muletensis* at the Jersey Wildlife Preservation Trust. – Dodo, **27**: 146–156.
- VALLS, J. A. O., X. MANZANO & S. PINYA (2014): Contando ferrets: 25 años de recuentos visuales de una especie en peligro de extinción. – Boletín de la Asociación Herpetológica Española, **25**: 37–43.
- VITT, L. J. & J. P. CALDWELL (2009): Herpetology. – Academic Press/Elsevier, Oxford, UK, 697 pp.
- VAN DER WESTHUIZEN, C. M. (1961): The development of the chondrocranium of *Heleophryne purcelli* Sclater with special reference to the palatoquadrate and the sound-conducting apparatus. – Acta Zoologica, **42**: 1–72.
- ZIERMANN, J. M. & L. OLSSON (2007): Patterns of spatial and temporal cranial muscle development in the African clawed frog, *Xenopus laevis* (Anura: Pipidae). – Journal of Morphology, **268**: 791–804.